Fluorescent Janus emulsions for biosensing of *Listeria monocytogenes*

Jie Li[a,b], Suchol Savagatrup[a,b], Zachary Nelson[a,b], Kosuke Yoshinaga[a,b], and Timothy M. Swager[a,b,1]

[a]Department of Chemistry, Massachusetts Institute of Technology, Cambridge, MA 02139; and [b]Institute for Soldier Nanotechnologies, Massachusetts Institute of Technology, Cambridge, MA 02139

Contributed by Timothy M. Swager, April 8, 2020 (sent for review February 11, 2020; reviewed by Mary J. Cloninger and Chad A. Mirkin)

Here we report a sensing method for *Listeria monocytogenes* based on the agglutination of all-liquid Janus emulsions. This two-dye assay enables the rapid detection of trace *Listeria* in less than 2 h via an emissive signal produced in response to *Listeria* binding. The biorecognition interface between the Janus emulsions is assembled by attaching antibodies to a functional surfactant polymer with a tetrazine/transcyclooctene click reaction. The strong binding between *Listeria* and the *Listeria* antibody located at the hydrocarbon surface of the emulsions results in the tilting of the Janus structure from its equilibrium position to produce emission that would ordinarily be obscured by a blocking dye. This method provides rapid and inexpensive *Listeria* detection with high sensitivity (<100 CFU/mL in 2 h) that can be paired with many antibody or related recognition elements to create a new class of biosensors.

Janus emulsion | fluorescent dyes | *Listeria monocytogenes* | biosensing | agglutination

Listeria is a genus of Gram-positive bacteria and is responsible for listeriosis, a potentially lethal foodborne bacterial illness (1–5). Listeriosis has a high mortality rate of 20 to 30%, and more than 90% of people with listeriosis are hospitalized; it is particularly dangerous for pregnant women and people with impaired immune systems (3, 6, 7). Water, fruits, vegetables, soil, and meat contaminated with *Listeria* are the primary sources of this disease (8). Efforts to mitigate the pathogen are frustrated by the fact that *Listeria* is a very robust class of bacteria with high environmental and temperature stress tolerance (1, 3, 9). As a result, *Listeria* detection methods with high sensitivity, rapid response time, and low cost are needed to ensure that these organisms are not distributed to the public in contaminated food (10, 11).

Dynamic complex droplets offer function that has been recognized for applications in drug delivery, food industry, and pharmaceutical formulations (12–22). They are also a versatile platform for biosensing enabling a combination of advantages including speed, portability, and cost effectiveness (23–27). Some droplet methods make use of morphology control using interfacial tensions and surfactants (28). The methods reported herein make use of complex droplets comprising equal volume of hydrocarbon and fluorocarbon oils in a Janus morphology, that spontaneously align in an equilibrium state as a result of differences in the density of the internal phases (13). Recognition elements attached to the surface of the hydrocarbon phase cause Janus droplets to agglutinate around their target, and bacteria can be detected by the resulting optical scattering from the agglutinated clusters (29). The detection of the degree of opacity and/or the number of agglutination events can be used in both qualitative and quantitative detection schemes. These attributes are attractive and can provide a generalizable sensor scheme for the detection of biomolecules, organisms or cells of interest. To create the most robust assays, we consider that a detection mode relying solely on optical scattering is insufficient for real-world samples containing particulates and could be interpreted as false positives.

In this paper, we employ a functional block copolymer surfactant that localizes at the interface of the continuous phase and the hydrocarbon phase of the droplets. The block copolymer (Poly-TCO) contains a hydrophobic polystyrene block with a high affinity for the hydrocarbon phase, a hydrophilic polyacrylic acid block, and a polyacrylic acid block that is partially conjugated with transcyclooctene (Fig. 1*A*). *Listeria* antibodies are functionalized through their free amines by reaction with tetrazine- *N*-hydroxysuccinimide (NHS) ester. Janus droplets prepared in phosphate buffered saline (PBS) buffer have Poly-TCO localized at the hydrocarbon-continuous phase interface (Figs. 1 *B* and *C*), and the tetrazine and transcyclooctene bioorthogonal reaction (30–37) is performed in situ. Detection is accomplished when the droplet immobilized antibodies bind multivalently to *Listeria* to cause clusters of tilted droplets, called agglutinations. The droplets microlens structure results in transmission of light with the Janus droplets transmitting in their equilibrium density-aligned states (26). The agglutination generates clusters of tilted droplets that are observed under a microscope, and counting these events gives a quantitative measure of the amount of *Listeria* in the solution.

To create a more robust system that will be immune from confounding debris that may be associated with real-world samples, we have designed a two-dye system (Fig. 1 *D* and *E*). The two dyes have orthogonal solubilities and improve the sensing performance by converting the agglutination into a turn-on emissive detection event. The choice of dyes is critical, and in the first scheme a subphthalocyanine (sub-PC) dye was designed to be exclusively soluble in the hydrocarbon phase and has a strong absorbance band that overlaps the emission band of a

Significance

***Listeria* has been a strong foodborne pathogen for years and can lead to severe diseases. Efficient sensing methods for quick detections of *Listeria* are still in demand. Here we designed a biosensor that installed *Listeria* antibodies on the surface of hydrocarbon phase of Janus droplets. We also dissolved a pair of blocking and emissive dyes in the hydrocarbon and fluorocarbon phases of Janus droplets. With the existence of *Listeria*, Janus droplets will form agglutinations and tilt that could be easily tracked by fluorimeter. Our work provides a sensitive, simple, and quick method for the detection of *Listeria*.**

Author contributions: J.L. and T.M.S. designed research; J.L., S.S., Z.N., and K.Y. performed research; Z.N. and K.Y. contributed new reagents/analytic tools; J.L., S.S., and T.M.S. analyzed data; and J.L., S.S., Z.N., K.Y., and T.M.S. wrote the paper.

Reviewers: M.J.C., Montana State University; and C.A.M., Northwestern University.

Competing interest statement: A patent has been filed on this technology under US Provisional Application No. 62/902,367, on September 18, 2019, "T. M. Swager, et al., Systems and methods for affecting interactions of electromagnetic radiation with Janus droplets for sensitive detection of species."

[1]To whom correspondence may be addressed. Email: tswager@mit.edu.

This article contains supporting information online at https://www.pnas.org/lookup/suppl/doi:10.1073/pnas.2002623117/-/DCSupplemental.

First published May 15, 2020.

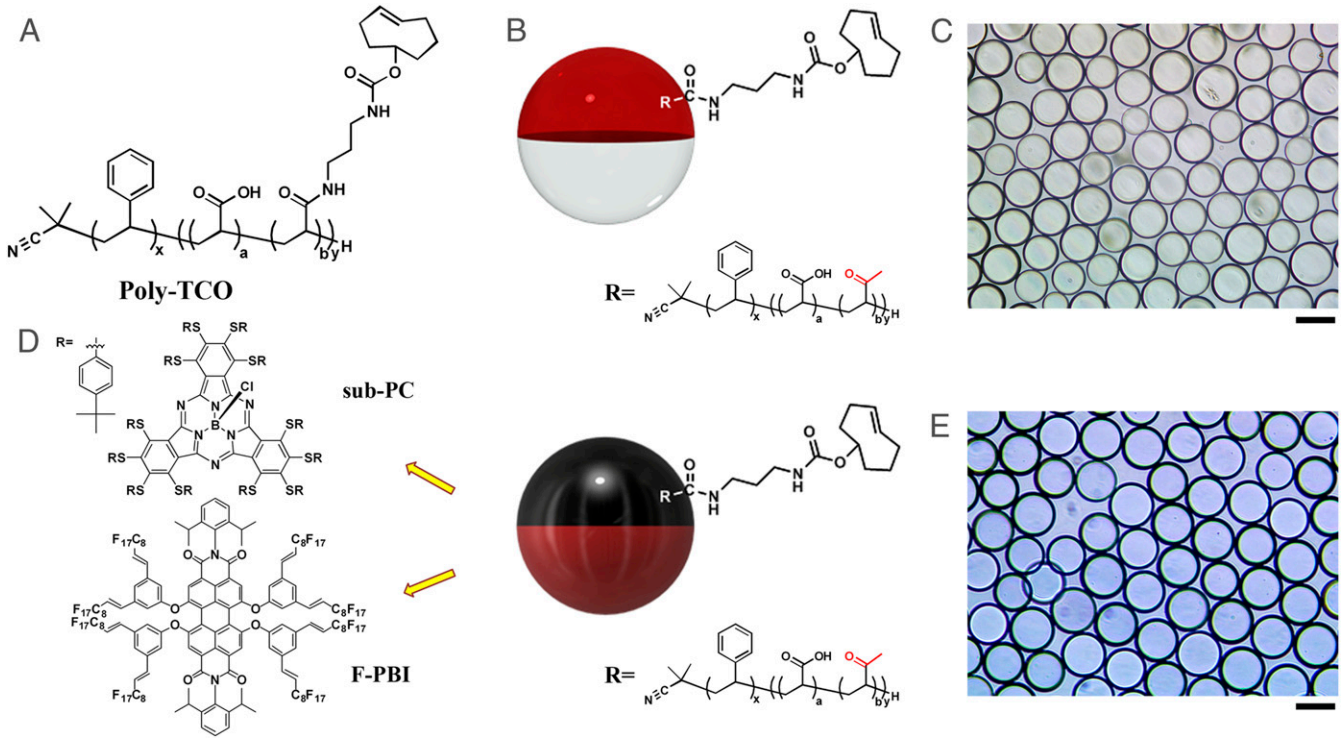

Fig. 1. (*A*) Chemical structure of Poly-TCO. (*B*) Scheme of Janus droplets containing 1 mg/mL of Poly-TCO in the hydrocarbon phase (red stands for hydrocarbon phase, and white stands for fluorocarbon phase). (*C*) Optical image (top view) of Janus droplets described in *B*. (*D*) Scheme of Janus droplet with Poly-TCO and sub-PC dye in the hydrocarbon phase and the F-PBI dye in the fluorocarbon phase (black stands for hydrocarbon phase with sub-PC, and dark red stands for fluorocarbon phase with F-PBI). The yellow arrows point out the structures of the dyes dissolved in each phase. (*E*) Optical image (top view) of Janus droplets described in *D*. (Scale bars, 50 μm.)

fluorous soluble PBI dye (F-PBI) (38) (Fig. 1*D*). In the absence of *Listeria*, the droplets align in the dish such that the fluorocarbon phase containing F-PBI is on the bottom and the hydrocarbon phase containing sub-PC is on the top due to the difference in density of the two liquids. In the aligned state, excitation and emission collection from the top give only a small signal from the F-PBI as a result of the absorptive blocking of both the excitation and emission of the F-PBI by the sub-PC dye in the top hydrocarbon phase. In contrast, when there is *Listeria* in the solution the resulting agglutinated tilted structure allows for unobstructed excitation of the F-PBI and the detection of its emission.

Results and Discussion

Preparation of Janus Emulsions and Bioconjugation at the Interfaces. Fig. 2*A* illustrates the synthesis of Poly-TCO. Polydisperse emulsion droplets containing Poly-TCO are obtained by dissolving 1 mg/mL of the polymer in diethylbenzene (DEB), addition of an equal volume of fluorocarbon solvent [3-ethoxyperfluoro(2-methylhexane) (HFE7500)] followed by dispersing (sonication) the mixture above the upper critical solution temperature at 40 °C in PBS buffer containing surfactants. Monodispersed droplets were fabricated using a microfluidic device with the same Poly-TCO/DEB/HFE7500 solution at temperatures above 40 °C. The postdroplet functionalization is illustrated in Fig. 2*B*. Twenty microliters of the droplet dispersion was transferred into a vial containing 0.5 mL of 0.1 wt % Zonyl:0.1 wt % Tween 20 1:1 (vol/vol) solution. Then 30 μL of tetrazine-*Listeria* antibody (1 mg/mL) was added to the continuous phase, and the mixture was mixed at room temperature on a rocker overnight to allow the transcyclooctene tetrazine bioconjugation. The unreacted tetrazine-*Listeria* antibody was subsequently removed by exchanging the continuous phase three times with 0.5 mL of fresh 0.1 wt % Zonyl:0.1 wt % Tween 20 1:1 (vol/vol) solution.

To confirm *Listeria* antibody bioconjugation, 5 μL of protein A-FITC (1 mg/mL), which has an affinity to the IgG *Listeria* antibody, is added to the continuous phase and mixed for 2 h on a rocker (Fig. 2*B*). The unbound protein A-FITC was removed by exchanging the continuous phase with 0.1 wt % Zonyl:0.1 wt % Tween 20 1:1 (vol/vol) solution for three times. The bright-field image shown in Fig. 2*C* reveals stable Janus droplets after the bioconjugation, and the confocal fluorescence imaging of the protein A-FTTC (Fig. 2*D*) confirms the successful bioconjugation of *Listeria* antibody at the hydrocarbon/continuous phase interface. Minor amounts of brightly fluorescent spots are also apparent on the droplet surfaces, which suggest the presence of aggregates formed from Poly-TCO, *Listeria* antibody, and protein A-FITC. The amount of *Listeria* antibody conjugated on droplets is quantified to be 3.7×10^{-10} mol m^{-2} by fluorescence spectra (*SI Appendix*, Fig. S1).

Agglutination Assay with Heat-Killed *Listeria monocytogenes*. After we validated the bioconjugation, we initiated sensing experiments by adding different concentrations of heat-killed *Listeria monocytogenes* to the continuous phase followed by mixing on a rocker for 2 h (Fig. 3*A*). To observe the orientational changes in the droplets, 10 μL of the droplet dispersion was added to 1 mL of 0.1 wt % Zonyl:0.1 wt % Tween 20 1:1 (vol/vol) solution in a Petri dish. An inverted microscope was used to record droplet agglutination (Fig. 3 *B*–*G* and *SI Appendix*, Fig. S18) after the addition of heat-killed *Listeria* at 10^7, 10^5, or 100 colony forming units (CFUs) per mL. Incubation time was set to be 2 h since with incubation time less than 2 h, we would get lower agglutination responses. Future optimization of mixing may potentially reduce the incubation time. Control experiments without the heat-killed *Listeria* or with equivalent amounts of *Bacillus subtilis*, heat-killed *Salmonella*, or BSA (Fig. 2*C* and *SI Appendix*, Figs. S19 and S20) showed no agglutination. The results shown in *SI Appendix*, Figs. S19 and S20, indicate

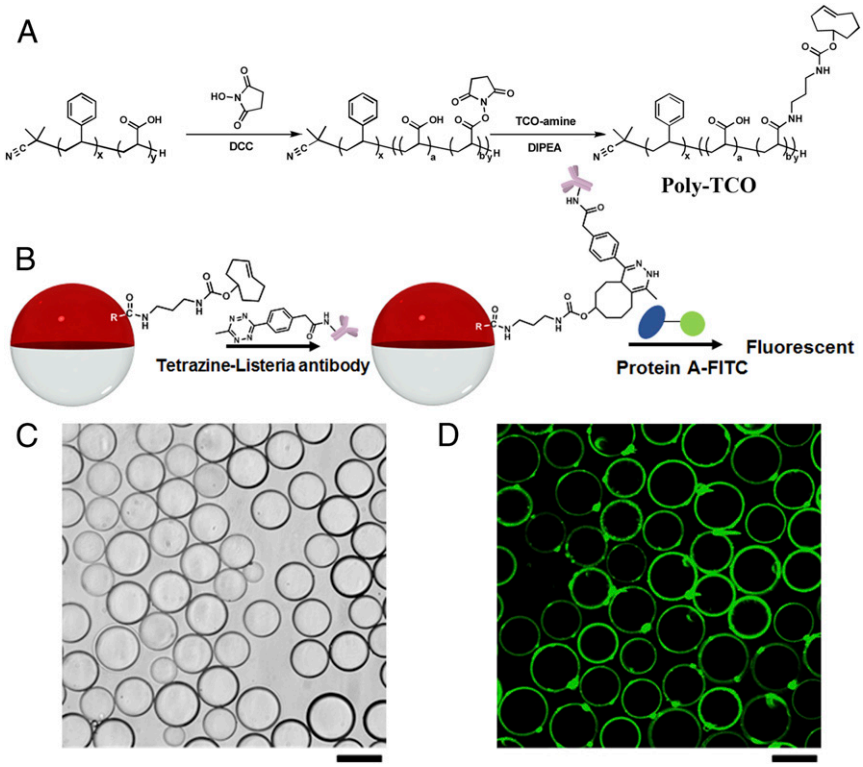

Fig. 2. (*A*) Synthetic route of Poly-TCO. (*B*) Postdroplet functionalization and protein A-FITC binding scheme. The violet shape is the symbol of Listeria antibody. (*C*) Bright-field microscope image of droplets with 1 mg/mL of Poly-TCO in the hydrocarbon phase after bioconjugation with tetrazine *Listeria* antibody. (*D*) Successful bioconjugation of *Listeria* antibody at the interface of droplets confirmed by fluorescent confocal microscopy. (Scale bars, 50 μm.)

that our sensing scheme shows excellent selectivity and specificity to *Listeria*. Agglutinations are readily observed at 100 CFUs per mL, thereby confirming limits of detection at this level or lower.

The quantification of the agglutinated droplets is performed using image analysis (see *SI Appendix* for more details). The image processing code transforms the optical micrographs into

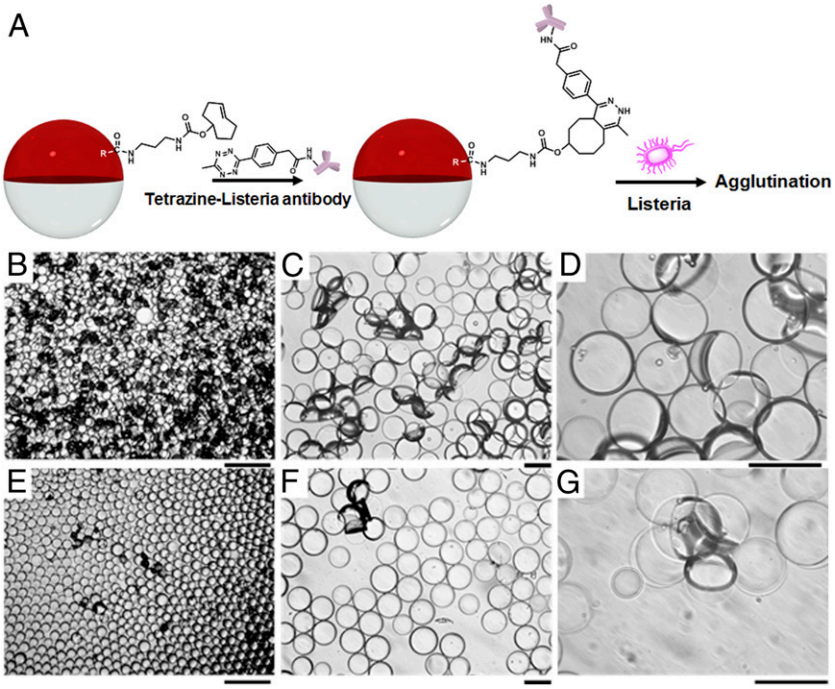

Fig. 3. (*A*) Heat-killed *L. monocytogenes* sensing scheme. (*B–G*) Optical images of droplets containing 1 mg/mL of Poly-TCO in the hydrocarbon phase after adding (*B–D*) 10^7 CFU/mL and (*E–G*) 100 CFU/mL of heat-killed *Listeria* for 2 h. (Scale bar of *B* and *E*, 200 μm; scale bar of *C*, *D*, *F*, and *G*, 50 μm.)

grayscale images and measures the average droplet diameters. To locate the agglutinated areas, the program first applies an adaptive thresholding algorithm, optimized on sets of images based on the original image contrast, and distinguishes the darker regions where multiple droplets are tilted off their natural axes (Fig. 4 *A*–*E*). Using the average droplet diameter and the area of the darker region, it then calculates the percentage of the agglutinated area of each image. Using this information, we can create a calibration curve that relates the percentage of agglutination increases with the number of heat-killed *L. monocytogenes* (Fig. 4*F*).

Quantification of Agglutination Using Two-Dye System. The methods just discussed made use of light transmission through Janus droplets and the modulation thereof by agglutination. To create more robust assays, we were interested in having agglutination produce new fluorescent signals on a dark or nearly dark background. This method could be used to facilitate the counting of agglutination events or allow for detection by monitoring of the total fluorescence. Field samples can contain random debris and/or waste from live organisms, which can potentially confound image analysis and light transmission-based assays. Hence, an emissive turn-on method has the prospects for avoiding false positive signals. To create such a scheme, we have developed water insoluble dyes with orthogonal solubilities between the hydrocarbon and fluorocarbon phase of Janus droplets. The sub-PC dye (*SI Appendix*, Figs. S2–S6) is only present in the DEB phase, whereas the emissive F-PBI dye (38) is localized exclusively in the fluorocarbon phase (Fig. 5*A*). This partitioning is apparent in the photos in Fig. 5*B*, whereas the sub-PC in the top DEB layer has dark green color, and the red F-PBI dye in the denser HFE7500 layer has strong emission after irradiation of UV light. From plotting the ratio of the molar absorptivity of the two dyes, we find blocking of the excitation light to be most efficient at 361 nm (*SI Appendix*, Figs. S7 and S8). Thus, we choose to excite the system at 361 nm.

Janus droplets align normal to a surface as a result of gravity and can be perturbed from this natural alignment by application of a magnetic field, by electrostatic interactions, or by chemical potentials (39–43). Our antibody conjugated droplets adopt this aligned state in the absence of their target analyte, and the sub-PC in the top hydrocarbon phase absorbs 361 nm light (*SI Appendix*, Fig. S7) thereby preventing the majority of light from reaching the bottom fluorocarbon phase (Fig. 1*D*). Some light will reach the fluorocarbon phase as a result of incomplete absorption or reflections. To further attenuate any fluorescence in the native aligned state, the dyes were chosen to have complementary absorption and emission characteristics. Specifically, F-PBI can be excited at 361 nm and has a strong emission at about 580 nm. The sub-PC has a very strong absorption at 580 nm with negligible emission. As a result, in the equilibrium alignment the sub-PC absorbs the excitation light as well as any emission from F-PBI, and the droplets appear dark. The data showing the filter effect are illustrated in Fig. 5*C* wherein the addition of the sub-PC dye reduces the F-PBI emission intensity by 17-fold (from 8,000 to 450 [arbitrary unit])

Agglutination of functionalized dye containing droplets results in a tilting and creates a path between the bifurcated fiber optic for excitation light and emitted light that does not need to pass through the sub-PC filter layer. Hence, the action of tilting the dyes from their surface normal orientation by agglutination produces an emission signal that can be monitored using a bifurcated fiber optic assembly as shown in Fig. 6*A*.

The responses of droplets functionalized with antibodies and containing dyes (Fig. 5*D*) were determined as a function of different concentrations of heat-killed *Listeria* with mixing for 2 h. Fig. 6*B* shows the emission spectra taken using the scheme in Fig. 6*A*. The calibration curve in Fig. 6*C* reveals a limit of detection less than 100 CFUs per mL. As expected, the emission at 580 nm increases with larger amounts of *Listeria*, in agreement with image analysis results shown in Fig. 4.

Emissive dyes can also be used with image analysis to create more robust methods. Specifically, the appearance of a new emission can differentiate from overlapping droplets or foreign objects that could be mistaken by image analysis as agglutination sites. This feature is illustrated by the images shown in Fig. 6 *D*–*G*. As can be seen, the agglutinated droplets are readily observed by the red F-PBI emission in Fig. 6 *E* and *G*, while the non-agglutinated droplets stay aligned normal, and little red F-PBI emission could be observed (Fig. 6 *D* and *F*).

Detection of Live *L. monocytogenes*. Similar to the previous sensing scheme, we added live *Listeria* (10^7, 10^4, and 100 CFUs per mL; Fig. 7 *A*–*C*) to the continuous phase and mixed the bacteria and droplets on a rocker for 2 h before taking images and fluorescence measurements. A high degree of agglutination was observed after adding 10^7 CFUs per mL of *Listeria*, and agglutination is still apparent after adding only 100 CFUs per mL of live *Listeria*. The detected emission of F-PBI dye at 580 nm increased with the

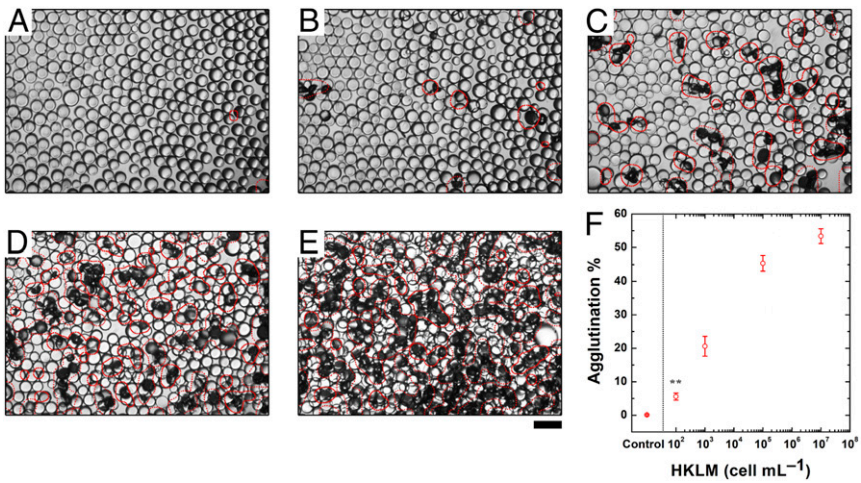

Fig. 4. (*A*–*E*) Optical images of droplets containing 1 mg/mL of Poly-TCO in the hydrocarbon phase after adding 0, 100, 10^3,10^5, or 10^7 CFU/mL of heat-killed *L. monocytogenes* for 2 h for processing algorithm for quantification of agglutination. The red markings on the optical micrographs signify the areas occupied by agglutinated droplets as a guide to the eye. (Scale bar, 100 μm.) (*F*) Correlation of heat-killed *L. monocytogenes* concentration and agglutination level (five replicate measurements were performed for the error bars, $^{**}P \leq 0.01$).

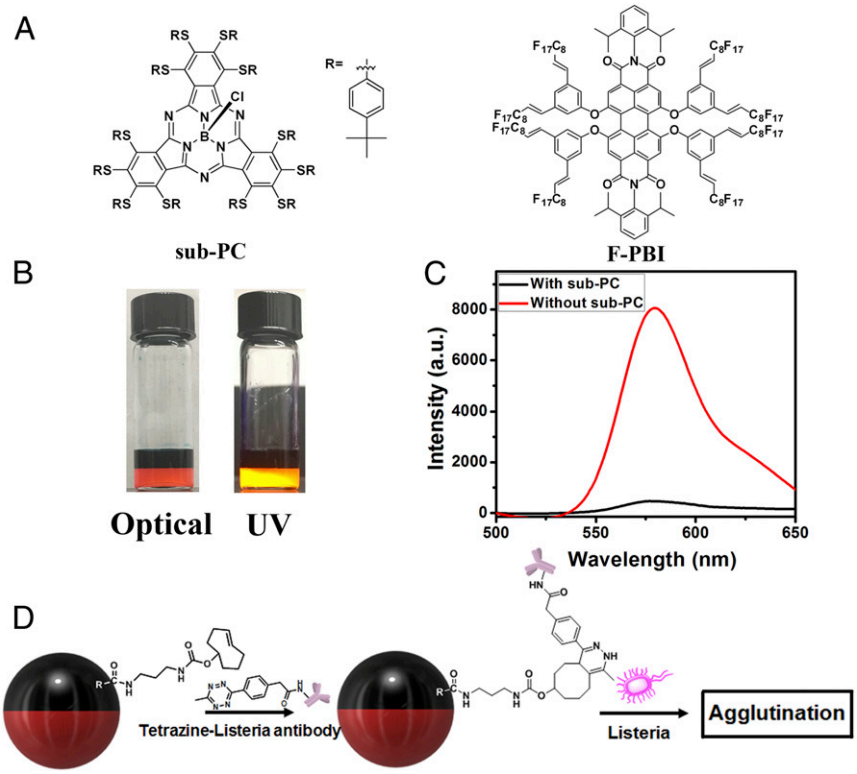

Fig. 5. (*A*) Chemical structures of a nonemissive sub-PC dye in the hydrocarbon phase (*Left*) and an emissive perylene dye (F-PBI) in the fluorocarbon phase (*Right*). (*B*) Optical images of the two-dye system (under normal or UV light). (*C*) Emission from Janus droplets aligned normal on a surface that have F-PBI in the fluorocarbon phase and have or lack the sub-PC dye in the hydrocarbon phase (λ_{ex} = 361 nm). (*D*) Postdroplet functionalization scheme of the two-dye system.

increase of the concentration of live *Listeria* (Fig. 7*D*), and a calibration curve in Fig. 7*E* confirms the ability to detect live *Listeria* at 100 CFUs per mL.

Inverted Two-Dye System. The arrangement of the dyes in the droplets need not be in form given in Fig. 1*D*, and in some cases an inverted arrangement of the blocking and signaling dyes has advantages. For example, in a highly scattering sample the emission could alternatively be detected from the bottom directly through a glass support, thereby eliminating the path length through the solution. This situation is accomplished as shown in Fig. 8*A*, wherein the perylene dye Lumogen F Orange 240 is exclusively soluble in the hydrocarbon phase. We synthesized a blocking subphthalocyanine dye (F-sub-PC) which is only soluble in the fluorocarbon phase (*SI Appendix*, Figs. S9–S15). The plot of ratio of the molar absorptivity of F-sub-PC and Lumogen F Orange 240 indicates that blocking of the excitation light to be most efficient at 398 nm (*SI Appendix*, Figs. S16 and S17), so that we excite the inverted two-dye system at 398 nm. The F-sub-PC dye absorbs the 398-nm excitation and the Lumogen F Orange 240 emission at 535 nm. The antibody functionalized droplet agglutination assay is conducted with the fiber optic under the glass container, and as shown in Fig. 8*B*, *Listeria* triggers an increased emission at 535 nm. The calibration curve suggests similar limit of detection of less than 100 CFUs per mL to the other methods (Fig. 8*C*).

Conclusions

In conclusion, we report a highly sensitive *Listeria* sensing method based on agglutination of Janus emulsion droplets with limits of detection less than 100 CFUs per mL in 2 h. Bioconjugation at the hydrocarbon phase-continuous phase interface of the droplets is accomplished by an efficient in situ click reaction between a tetrazine conjugated *Listeria* antibody and a transcyclooctene surfactant polymer. Exposure to *Listeria* induced agglutination and tilting of the droplets from their natural gravity-induced alignment which could be quantified by image analysis. More robust agglutination assays are created using blocking and emissive dyes that are orthogonally partitioned between the hydrocarbon and fluorocarbon phases of the Janus droplet. These methods make use of an emission turn-on triggered by agglutination which may be monitored from the top or the bottom with the proper selection of blocking and emissive dyes. Assays monitoring from the bottom have the advantage that highly scattering solutions can be used because the emission signal need not travel through the solution. These droplet methods are robust and are stable in serum, synthetic blood, and brain heart infusion broth which guarantees the future applications in biomedical or biochemistry fields (*SI Appendix*, Figs. S21–S24). Through enrichment process, we could easily detect 20 CFUs per mL of *Listeria* after incubating it at 37 °C for 4 h (*SI Appendix*, Fig. S25). We could also get enhanced signal of 100 CFUs per mL of *Listeria* by incubating it at 37 °C for up to 12 h and the relative intensity at 580 nm increase with the increase of incubation time (*SI Appendix*, Fig. S26). Our method is simple and convenient, and agglutinations could even be detected by a smartphone camera with a magnifying lens (*SI Appendix*, Figs. S27 and S28). The effects we report can be detected in some cases by visual inspection. Specifically agglutination induces strong fluorescence in the sub-PC/F-PBI system when the excitation is performed under total internal reflection conditions using a glass prism at the glass interface (*SI Appendix*, Fig. S29) (44, 45). The present assays readily achieve a detection limit of *Listeria* of 100 CFUs per mL and can be extended to the detection of different analytes by the utilization of corresponding stable and selective antibodies.

Materials and Methods

Materials. All chemical reagents and solvents were purchased from Sigma-Aldrich, ThermoFisher, Combi-Blocks, Click Chemistry Tools, BroadPharm, or

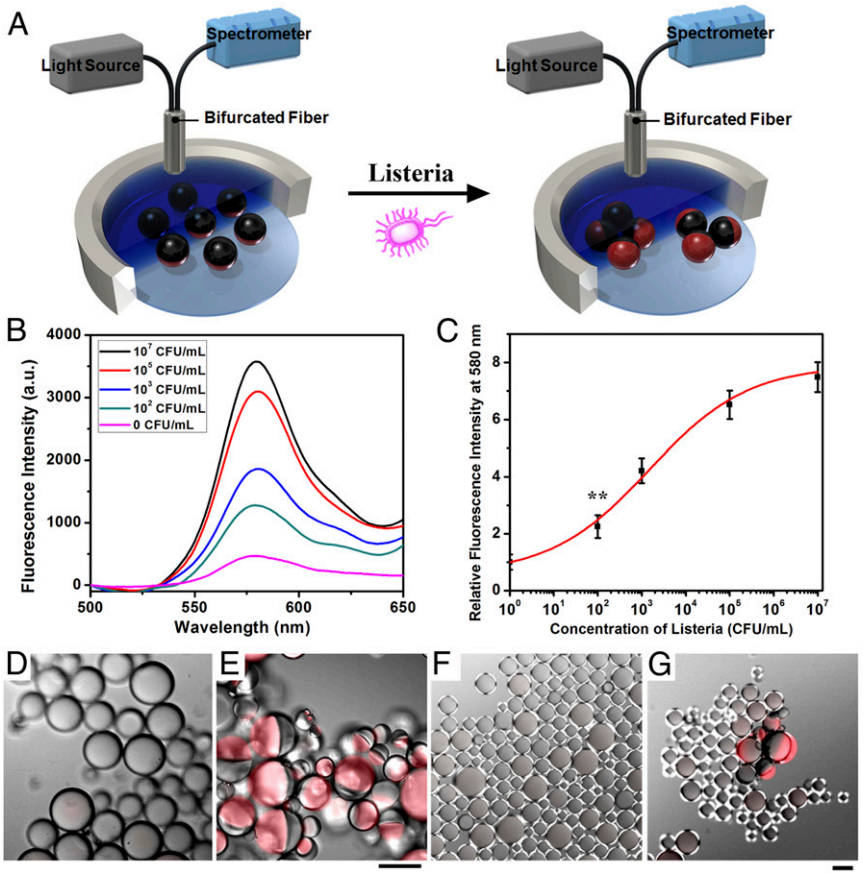

Fig. 6. (*A*) Measurement scheme showing excitation and monitoring of the fluorescence coming from the dyed emulsions. (*B*) Fluorescence spectra (λ_{ex} = 361 nm) of droplet containing Poly-TCO and sub-PC dye in the hydrocarbon phase and F-PBI dye in the fluorocarbon phase after addition of heat-killed *Listeria* at different concentrations. (*C*) Correlation of concentration of heat-killed *Listeria* and relative fluorescence intensity at 580 nm (three replicate measurements were performed for the error bars, $^{**}P \leq 0.01$). (*D* and *E*) Confocal microscope image of (*D*) nonagglutinated droplet (without addition of *Listeria*) and (*E*) agglutinated droplets (with the addition of *Listeria* at 10^7 CFU/mL). (*F* and *G*) Confocal microscope image of (*F*) nonagglutinated droplet (without addition of *Listeria*) and (*G*) agglutinated droplets (with the addition of *Listeria* at 100 CFU/mL), with sub-PC dye in the hydrocarbon phase and F-PBI dye in the fluorocarbon phase. (Scale bars, 50 μm.)

TCI. Unless stated otherwise, all chemicals were of reagent grade and used as received. Heat-killed *L. monocytogenes* was purchased from InvivoGen, and *L. monocytogenes* was purchased from ATCC. All air- and water-sensitive synthetic manipulations were performed in oven-dried glassware under an argon atmosphere using standard Schlenk techniques.

Bulk Emulsification Method for Preparing Droplets. We utilized our previously published method to prepare polydispersed droplets (46). Diethylbenzene (DEB, hydrocarbon phase) and 3-ethoxyperfluoro(2-methylhexane) (HFE7500, fluorocarbon phase) were mixed at a 1:1 ratio in a 4-mL vial. The mixture was heated above 40 °C, which is the temperature that the two phases become miscible. These polydispersed droplets were produced by adding 20 μL of warm DEB–HEF7500 liquid into 500 μL of warm surfactant solution (a mixture of 0.1 wt % Zonyl:0.1 wt % Tween 20 1:1 [vol/vol]), and shaking the mixture on a Vortex for 10 s. To generate emulsion droplets containing Poly-TCO for interfacial functionalization, Poly-TCO was dissolved at 1 mg/mL in DEB.

Preparation of Monodispersed Droplets. Continuous phase (1.0 wt % tween 20) and the 1:1 ratio mixture of hydrocarbon phase (containing 1 mg/mL Polymer-TCO) and fluorocarbon phase were pumped into a chip at a diameter of 50 μm to get monodispersed droplets with a diameter of 50 μm at 40 °C. The monodispersed droplets were then washed with the mixture of 0.1 wt % Zonyl:0.1 wt % Tween 20 1:1 (vol/vol) solution for three times to get Janus droplets.

Preparation of Droplet Containing Two Dyes. Subphthalocyanine was dissolved in diethylbenzene at concentration of 1 mM, and the perylene dye, F-PBI, was dissolved in HFE7500 at concentration of 0.1 mM. Poly-TCO was dissolved in diethylbenzene at concentration of 1 mg/mL. The continuous aqueous phase was a mixture of 0.1 wt % Zonyl:0.1 wt % Tween 20 1:1 (vol/vol).

For the inverted phase droplets, Lumogen F Orange 240 was dissolved in diethylbenzene at concentration of 0.1 mM, and Poly-TCO was dissolved in diethylbenzene at concentration of 1 mg/mL. F-sub-PC was dissolved in HFE7500 at concentration of 1 mM. The continuous aqueous phase was a mixture of 0.1 wt % Zonyl:0.1 wt % Tween 20 1:1 (vol/vol).

Quantification of *Listeria* Antibody. We prepared monodispersed droplets containing 1 mg/mL poly-TCO in the hydrocarbon phase with a diameter of 50 μm. Thirty microliters of tetrazine-*Listeria* antibody (1 mg/mL) was added to the continuous phase of droplet, and the mixture was mixed at room temperature overnight. We washed the droplets with a mixture of 0.1 wt % Zonyl:0.1 wt % Tween 20 1:1 (vol/vol) for three times to remove the unconjugated tetrazine *Listeria* antibody. Then 5 μL of protein A-FITC (1 mg/mL) was added to the continuous phase for 2 h at room temperature. We washed the droplets with a mixture of 0.1 wt % Zonyl:0.1 wt % Tween 20 1:1 (vol/vol) for three times to remove the unbound protein A-FITC. We counted the number of monodispersed droplets and then dried all of the droplets in a 4-mL vial. We added 2 mL of DI water to redissolve the protein A-FITC released from the dried droplets. Fluorescence spectrum was measured with excitation at 490 nm, and its emission at 518 nm was 2,830 (*SI Appendix*, Fig. S1*C*). Calibration curve was measured by measuring the fluorescence spectra of protein A-FITC at 0.1, 0.05, 0.02, 0.01 and 0.005 μg/mL (*SI Appendix*, Fig. S1 *A* and *B*). The equation of calibration curve is

$$y = 164{,}245x + 177.$$

Using this calibration equation, we could calculate that the protein A-FITC concentration of the redissolved solution should be 0.016 μg/mL. Since

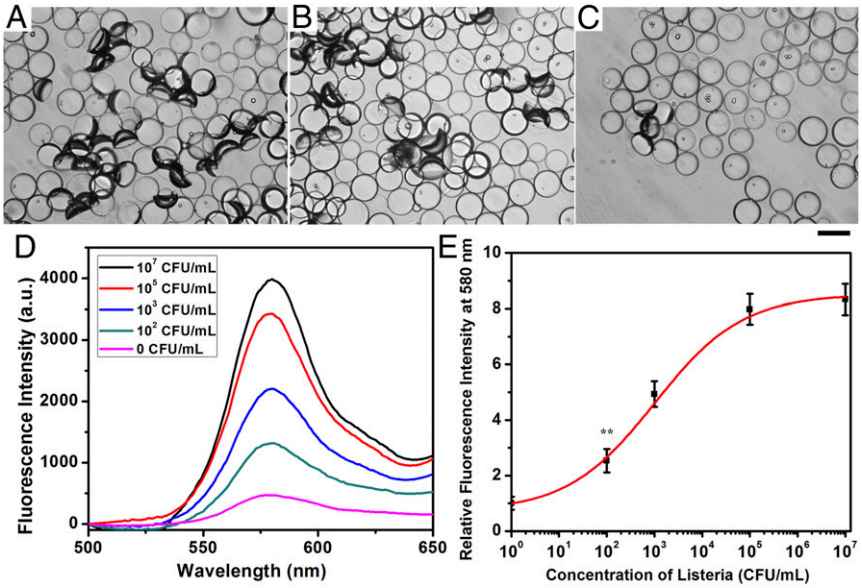

Fig. 7. Optical images of droplets containing 1 mg/mL of Poly-TCO in the hydrocarbon phase after adding (*A*) 10^7 CFU/mL, (*B*) 10^4 CFU/mL, and (*C*) 100 CFU/mL of live *Listeria* for 2 h. (Scale bar, 50 μm.) (*D*) Fluorescence spectra (λ_{ex} = 361 nm) of droplets containing Poly-TCO and sub-PC dye in the hydrocarbon phase and F-PBI dye in the fluorocarbon phase after addition of live *Listeria* at different concentrations. (*E*) Correlation of concentration of live *Listeria* and relative fluorescence intensity at 580 nm (three replicate measurements were performed for the error bars, $^{**}P \leq 0.01$).

protein A-FITC was bound to *Listeria* antibody on the surface of Janus droplets, the number of *Listeria* antibody should be equal to or larger than the number of protein A-FITC. Given that the molecular weight of protein A-FITC is 56 kDa and the number of the dried monodispersed droplet is 4×10^5, we calculated that the number of protein A-FITC per droplet is 8.5×10^5. Thus, the number of *Listeria* antibodies per droplet is at or higher than 8.5×10^5. The diameter of the droplet is 50 μm, so after calculation, the surface area of hydrocarbon of one Janus droplet (hemisphere) is 3.9 × 10^9 nm^2, and the

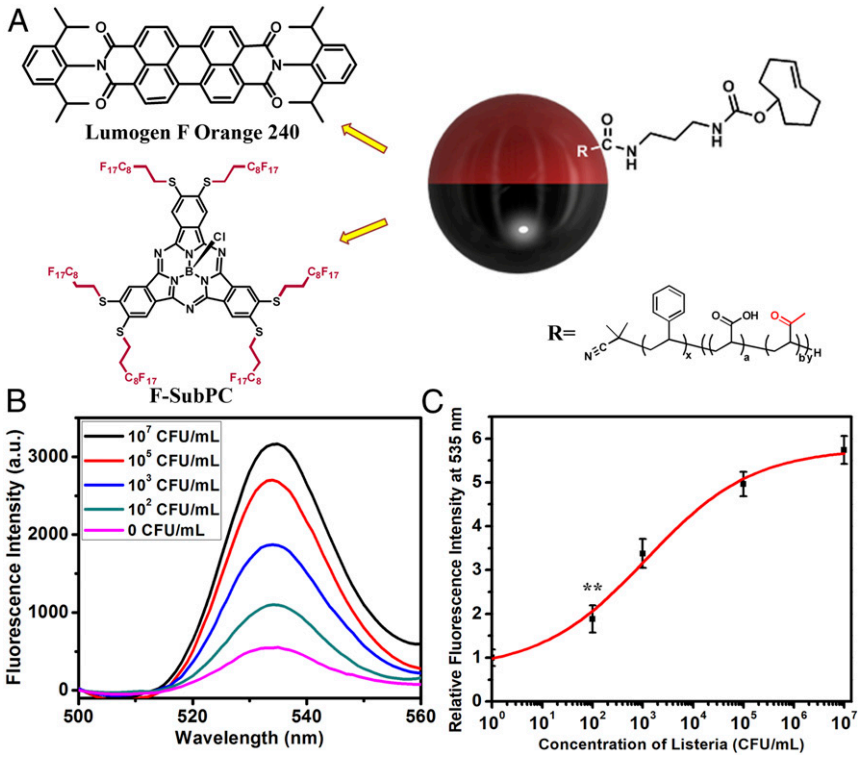

Fig. 8. (*A*) Janus droplet having a subphthalocyanine dye (F-Sub-PC) in the fluorocarbon phase and an emissive PBI dye (Lumogen F Orange 240) in the hydrocarbon phase. The dyes are exclusively insoluble in the phases that they are not shown in. (*B*) Fluorescence spectra (λ_{ex} = 398 nm) of droplets containing Poly-TCO and Lumogen F Orange 240 in the hydrocarbon phase and F-sub-PC dye in the fluorocarbon phase after addition of *Listeria* at different concentrations. (*C*) Correlation of concentration of *Listeria* and relative fluorescence intensity at 535 nm (three replicate measurements were performed for the error bars, $^{**}P \leq 0.01$).

number of antibodies on droplet is at or higher than 2.2×10^{14} per m^2, which is 3.7×10^{-10} mol per m^2. The area per *Listeria* antibody on the surface of droplet is 4,600 nm^2 per antibody.

***Listeria* Cell Culture.** *Listeria* strain 19115 was grown in brain heart infusion (BHI) broth in a 50-mL tube overnight at 37 °C in an incubator. After they reached an approximate OD600 of 1.0, the culture was centrifuged at 5,000 rpm for 10 min. The cells were washed with 15 mL of PBS buffer, and the procedure was repeated for three times. CFUs of live *Listeria* were quantified by colony counting method. We diluted the *Listeria* solution by different dilution factors and added 10 μL of these dilutions onto a BHI agar dish for growth at 37 °C for overnight. The original *Listeria* solution was stored at 4 °C to prevent further growth. After the formation of colonies, we counted the number of colonies by a magnifying glass. We could use these colony numbers and the dilution factors to calculate the CFU of the original *Listeria* solution. Growth curves of *Listeria* were measured by quantifying the CFUs of growing *Listeria*. We cultured *Listeria* in an incubator at 37 °C and took out 1 mL aliquot from the *Listeria* culture tube every 2 h. We quantified the CFUs of these aliquots and plot the growth curves with the quantified CFUs. To conduct live *Listeria* tests, a 10-μL aliquot of cells was added to the Janus emulsion assay.

Correlation Curves. We have performed three replicate measurements for the experiments shown in Figs. 6–8 and five replicate measurements for the experiment shown in Fig. 4. These measurements were done directly without further enrichments.

Synthesis of Poly-TCO. One hundred milligrams of polystyrene-block-poly (acrylic acid) was dissolved in 20 mL of DCM; 72 mg of NHS and 120 mg of N,N′-Dicyclohexylcarbodiimide (DCC) were added into the solution and stirred overnight at room temperature. The reaction mixture was then precipitated into 150 mL water. The product (polymer-NHS) was washed with methanol, acetone, and hexane after filtration. Then we dissolved 30 mg of polymer-NHS in DCM, added 0.03 mL of N,*N*-Diisopropylethylamine (DIPEA) and 9 mg of TCO-amine Hydrochloride into the solution, and stirred at room temperature for overnight. The reaction mixture was then precipitated into 100 mL water. The product (Poly-TCO) was washed with methanol, acetone, and hexane after filtration.

Synthesis of Sub-PC and F-sub-PC. Sub-PC and F-sub-PC are synthesized and characterized. Please see *SI Appendix* for more details.

Data Availability. The data presented in this manuscript are available in the *SI Appendix*.

ACKNOWLEDGMENTS. This research was supported by a Vannevar Bush Faculty Fellowship to T.M.S. (Grant N000141812878). This research was also supported by NSF Center for Energy Efficient Electronics Science (Award ECCS-0939514). S.S. was supported by an F32 Ruth L. Kirschstein National Research Service Award. K.Y. thanks Funai Overseas Scholarship for financial support.

1. J. M. Farber, P. I. Peterkin, Listeria monocytogenes, a food-borne pathogen. *Microbiol. Rev.* **55**, 476–511 (1991).
2. J. A. Vázquez-Boland *et al*., Listeria pathogenesis and molecular virulence determinants. *Clin. Microbiol. Rev.* **14**, 584–640 (2001).
3. P. S. Mead *et al*., Food-related illness and death in the United States. *Emerg. Infect. Dis.* **5**, 607–625 (1999).
4. C. S. Hsieh *et al*., Development of TH1 CD4+ T cells through IL-12 produced by Listeria-induced macrophages. *Science* **260**, 547–549 (1993).
5. S. Boatemaa *et al*., Awakening from the listeriosis crisis: Food safety challenges, practices and governance in the food retail sector in South Africa. *Food Control* **104**, 333–342 (2019).
6. E. Scallan *et al*., Foodborne illness acquired in the United States—Major pathogens. *Emerg. Infect. Dis.* **17**, 7–15 (2011).
7. M. Hamon, H. Bierne, P. Cossart, Listeria monocytogenes: A multifaceted model. *Nat. Rev. Microbiol.* **4**, 423–434 (2006).
8. S. Burt, Essential oils: Their antibacterial properties and potential applications in foods—A review. *Int. J. Food Microbiol.* **94**, 223–253 (2004).
9. R. L. Scharff, Economic burden from health losses due to foodborne illness in the United States. *J. Food Prot.* **75**, 123–131 (2012).
10. S. Alhogail, G. A. R. Y. Suaifan, M. Zourob, Rapid colorimetric sensing platform for the detection of Listeria monocytogenes foodborne pathogen. *Biosens. Bioelectron.* **86**, 1061–1066 (2016).
11. D. K. Soni, R. Ahmad, S. K. Dubey, Biosensor for the detection of Listeria monocytogenes: Emerging trends. *Crit. Rev. Microbiol.* **44**, 590–608 (2018).
12. M. A. Augustin, Y. Hemar, Nano- and micro-structured assemblies for encapsulation of food ingredients. *Chem. Soc. Rev.* **38**, 902–912 (2009).
13. J. Zhang, B. A. Grzybowski, S. Granick, Janus particle synthesis, assembly, and application. *Langmuir* **33**, 6964–6977 (2017).
14. S.-H. Hu, S.-Y. Chen, X. Gao, Multifunctional nanocapsules for simultaneous encapsulation of hydrophilic and hydrophobic compounds and on-demand release. *ACS Nano* **6**, 2558–2565 (2012).
15. Y. Jia *et al*., Electrically controlled rapid release of actives encapsulated in double-emulsion droplets. *Lab Chip* **18**, 1121–1129 (2018).
16. J. Forth *et al*., Building reconfigurable devices using complex liquid-fluid interfaces. *Adv. Mater.* **31**, e1806370 (2019).
17. Z. Nie, W. Li, M. Seo, S. Xu, E. Kumacheva, Janus and ternary particles generated by microfluidic synthesis: Design, synthesis, and self-assembly. *J. Am. Chem. Soc.* **128**, 9408–9412 (2006).
18. R. G. McAllister, H. Metwally, Y. Sun, L. Konermann, Release of native-like gaseous proteins from electrospray droplets via the charged residue mechanism: Insights from molecular dynamics simulations. *J. Am. Chem. Soc.* **137**, 12667–12676 (2015).
19. D. Suzuki, S. Tsuji, H. Kawaguchi, Janus microgels prepared by surfactant-free pickering emulsion-based modification and their self-assembly. *J. Am. Chem. Soc.* **129**, 8088–8089 (2007).
20. J. Wadhwa, A. Nair, R. Kumria, Emulsion forming drug delivery system for lipophilic drugs. *Acta Pol. Pharm.* **69**, 179–191 (2012).
21. D. Lee, D. A. Weitz, Double emulsion-templated nanoparticle colloidosomes with selective permeability. *Adv. Mater.* **20**, 3498–3503 (2008).
22. V. Jokinen, L. Sainiemi, S. Franssila, Complex droplets on chemically modified silicon nanograss. *Adv. Mater.* **20**, 3453–3456 (2008).
23. L. D. Zarzar, J. A. Kalow, X. He, J. J. Walish, T. M. Swager, Optical visualization and quantification of enzyme activity using dynamic droplet lenses. *Proc. Natl. Acad. Sci. U.S.A.* **114**, 3821–3825 (2017).
24. M. Yoshida *et al*., Structurally controlled bio-hybrid materials based on unidirectional association of anisotropic microparticles with human endothelial cells. *Adv. Mater.* **21**, 4920–4925 (2009).
25. L. Zeininger *et al*., Rapid detection of *Salmonella enterica* via directional emission from carbohydrate-functionalized dynamic double emulsions. *ACS Cent. Sci.* **5**, 789–795 (2019).
26. S. Nagelberg *et al*., Reconfigurable and responsive droplet-based compound microlenses. *Nat. Commun.* **8**, 14673 (2017).
27. Q. Zhang, S. Savagatrup, P. Kaplonek, P. H. Seeberger, T. M. Swager, Janus emulsions for the detection of bacteria. *ACS Cent. Sci.* **3**, 309–313 (2017).
28. L. D. Zarzar *et al*., Dynamically reconfigurable complex emulsions via tunable interfacial tensions. *Nature* **518**, 520–524 (2015).
29. Q. Zhang *et al*., Emulsion agglutination assay for the detection of protein-protein interactions: An optical sensor for Zika virus. *ACS Sens.* **4**, 180–184 (2019).
30. M. L. Blackman, M. Royzen, J. M. Fox, Tetrazine ligation: Fast bioconjugation based on inverse-electron-demand Diels-Alder reactivity. *J. Am. Chem. Soc.* **130**, 13518–13519 (2008).
31. N. K. Devaraj, R. Weissleder, Biomedical applications of tetrazine cycloadditions. *Acc. Chem. Res.* **44**, 816–827 (2011).
32. K. Lang, J. W. Chin, Cellular incorporation of unnatural amino acids and bioorthogonal labeling of proteins. *Chem. Rev.* **114**, 4764–4806 (2014).
33. M. D. Best, Click chemistry and bioorthogonal reactions: Unprecedented selectivity in the labeling of biological molecules. *Biochemistry* **48**, 6571–6584 (2009).
34. M. T. Taylor, M. L. Blackman, O. Dmitrenko, J. M. Fox, Design and synthesis of highly reactive dienophiles for the tetrazine-trans-cyclooctene ligation. *J. Am. Chem. Soc.* **133**, 9646–9649 (2011).
35. R. Selvaraj, J. M. Fox, trans-Cyclooctene—A stable, voracious dienophile for bioorthogonal labeling. *Curr. Opin. Chem. Biol.* **17**, 753–760 (2013).
36. J. L. Seitchik *et al*., Genetically encoded tetrazine amino acid directs rapid site-specific in vivo bioorthogonal ligation with trans-cyclooctenes. *J. Am. Chem. Soc.* **134**, 2898–2901 (2012).
37. K. M. El Muslemany *et al*., Photoactivated bioconjugation between ortho-azidophenols and anilines: A facile approach to biomolecular photopatterning. *J. Am. Chem. Soc.* **136**, 12600–12606 (2014).
38. K. Yoshinaga, T. M. Swager, Fluorofluorescent perylene bisimides. *Synlett* **29**, 2509–2514 (2018).
39. V. B. Varma *et al*., Control of ferrofluid droplets in microchannels by uniform magnetic fields. *IEEE Magn. Lett.* **7**, 1–5 (2016).
40. X. Hong, X. Gao, L. Jiang, Application of superhydrophobic surface with high adhesive force in no lost transport of superparamagnetic microdroplet. *J. Am. Chem. Soc.* **129**, 1478–1479 (2007).
41. T. Ohashi, H. Kuyama, K. Suzuki, S. Nakamura, Control of aqueous droplets using magnetic and electrostatic forces. *Anal. Chim. Acta* **612**, 218–225 (2008).
42. P. Mulvaney, J. M. Perera, S. Biggs, F. Grieser, G. W. Stevens, The direct measurement of the forces of interaction between a colloid particle and an oil droplet. *J. Colloid Interface Sci.* **183**, 614–616 (1996).
43. S. Y. Teh, R. Lin, L. H. Hung, A. P. Lee, Droplet microfluidics. *Lab Chip* **8**, 198–220 (2008).
44. L. Zeininger *et al*., Waveguide-based chemo- and biosensors: Complex emulsions for the detection of caffeine and proteins. *Lab Chip* **19**, 1327–1331 (2019).
45. C. McDonagh, C. S. Burke, B. D. MacCraith, Optical chemical sensors. *Chem. Rev.* **108**, 400–422 (2008).
46. Q. Zhang, A. Scigliano, T. Biver, A. Pucci, T. M. Swager, Interfacial bioconjugation on emulsion droplet for biosensors. *Bioorg. Med. Chem.* **26**, 5307–5313 (2018).